



The University of Bradford Institutional Repository

<http://bradscholars.brad.ac.uk>

This work is made available online in accordance with publisher policies. Please refer to the repository record for this item and our Policy Document available from the repository home page for further information.

To see the final version of this work please visit the publisher's website. Access to the published online version may require a subscription.

Link to publisher's version: <http://dx.doi.org/10.1111/1556-4029.13523>

Citation: Bukar AM and Ugail H (2017) Facial age synthesis using sparse partial least squares (the case of Ben Needham). *Journal of Forensic Sciences*. 62(5): 1205-1212.

Copyright statement: © 2017 American Academy of Forensic Sciences.

This is the peer reviewed version of the following article: Bukar AM and Ugail H (2017) Facial age synthesis using sparse partial least squares (the case of Ben Needham). *Journal of Forensic Sciences*. 62(5): 1205-1212, which has been published in final form at [<http://dx.doi.org/10.1111/1556-4029.13523>]. This article may be used for non-commercial purposes in accordance with Wiley Terms and Conditions for Self-Archiving.

Facial Age Synthesis Using Sparse Partial Least Squares (The Case of Ben Needham)

A.M. Bukar (MSc) and H. Ugail (Ph.D.)

Centre for Visual Computing, University of Bradford,
Bradford BD7 1DP, United Kingdom.

ambukar@student.bradford.ac.uk (corresponding author) and h.ugail@bradford.ac.uk

Abstract

Automatic facial age progression (AFAP) has been an active area of research in recent years. This is due to its numerous applications which include searching for missing. This study presents a new method of AFAP. Here, we use an Active Appearance Model (AAM) to extract facial features from available images. An ageing function is then modelled using Sparse Partial Least Squares Regression (sPLS). Thereafter, the ageing function is used to render new faces at different ages. To test the accuracy of our algorithm, extensive evaluation is conducted using a database of 500 face images with known ages. Furthermore, the algorithm is used to progress Ben Needham's facial image that was taken when he was 21 months old to the ages of 6, 14 and 22 years. The algorithm presented in this paper could potentially be used to enhance the search for missing people worldwide.

Keywords: forensic science, age estimation, age synthesis, active appearance model, sparse partial least squares regression, age progression, Ben Needham

The Case of Ben Needham is claimed to be one of the longest missing person's case in British history. Born in Sheffield, on 29th of October 1989, Ben Needham disappeared while on holiday with his parents in the Greek island of Kos on 24th July 1991, when he was only 21 months old (1).

Ben went missing in the village of Iraklise, where his maternal grandparents had migrated. On the day of his disappearance, Ben's mother was in her workplace in a local hotel (Palm Beach Hotel), while he was left in the care of his grandparents. He was seen playing with his toy cars in the mud and splashing water around a farmhouse the family were renovating, when around 2.30 PM, it was realised he had disappeared (1).

The family first searched the area, assuming Ben had wandered off, or that his teenage uncle, Stephen, had taken him out. When no traces of him could be found, the police were notified. However, the police blamed Ben's grandparents, and extensively questioned them as prime suspects. As a result, the search for Ben was very local [5], but eventually, the police widened their search to investigate the disappearance.

In 2003, shortly before the twelfth anniversary of Ben's disappearance, the Metropolitan Police Facial Imaging Team created an updated photograph of Ben using age progression techniques to alter his toddler picture. This was done in order to predict how he would look when he was thirteen years old.

In 2011, there was an excitement for the search when South Yorkshire Police agreed to work with the Greek authorities to reopen the case. To date, despite numerous false sightings over the years, no trace of the British toddler has ever been found. However, Ben's mother Kerry, continues to hope that someday he would be found.

Recently automatic facial ageing (AFA) has gained popularity due to its numerous applications; the most obvious has been for the search of missing people. Advancements in this area have been discussed in comprehensive reviews such as Fu et al. (2). Although recent progress has been made in this case, no conclusive evidence has been found. Furthermore, motivated by the fact that each year the police record approximately 300, 000 missing person cases in the UK

alone (3), we endeavour to improve the current techniques of searching for missing people in order to achieve more successful outcomes. We present a novel age synthesis framework which revisits the approach we discussed in (4).

Our contribution, in this paper, includes the presentation of a computer based method using Sparse Partial Least Squares Regression for age estimation. Then, face synthesis is undertaken via a linear algebraic approach which inverts the age estimator. Finally, using rigorous evaluation procedures, we compare the synthesised images to those produced by the Metropolitan Police Facial Imaging Team. This comparison is primarily done as a form of evaluation of the quality of our results. We would like to highlight that this work is not geared in any way to criticise the existing police work. Rather, we are presenting our results as a form of improvement on the synthesised images released by the Police.

Related Work

Age Progression

Age synthesis, also called age progression, involves the automatic reconstruction of a human face with natural ageing effects (2). This area of automatic facial analysis has been very active over the last 15 years (5). This is due to its practical applications which include searching for missing people and the identification of fugitives.

The earliest method used for age progression is the forensic artist's approach. Here the subject's image, in combination with images of his/her relatives, as well as additional information such as life style, are used to render the picture as an artistic hand sketch. Alternatively, a computer based graphic drawing approach guided by the knowledge of the forensic artist can be applied (6). The former is still predominantly used by police departments around the world. While the method has been successful in the past, it requires remarkable talent and years of experience. Normally the forensic artist undergoes thorough training and requires a good knowledge of interviewing procedures, behavioural science, cognitive psychology and craniofacial anthropometry (6).

As stated earlier, facial ageing has gained interest among computer vision researchers. Hence, several methods have been proposed in the literature. According to Fu et al. (2), automatic facial ageing can be categorised based on the face modelling techniques. These include geometric, image based and statistical learning approaches. Geometric techniques model the face via geometric primitives. Examples include, anthropometric models (7), parametric active contours (8), dynamic muscle modelling (9) and structured facial mesh (10). In general, geometric models render non-photo realistic images. Thus, they are better suited for computer animation, caricaturing and cartooning.

Image based models render photo realistic faces via manipulation of the facial texture details such skin wrinkles. Ageing has been simulated by independent wrinkle generation (11) or by transferring wrinkles across faces (12). Age estimation using 3D wrinkle formation has also been proposed (13). Studies have shown that texture changes are more obvious after adulthood (2). Hence, image-based synthesis cannot be generalised across all age groups.

Statistical Learning methods consider both shape and texture either separately or in a combined form. Facial variations, such as shape and texture, are learnt from a large database of faces. Thus, each face is regarded as a high dimensional point in the age space. The most popular models used are the Active Appearance Models (AAM) (14) and 3D Morphable Models (15). In the work of Lanitis et al. (16), for example, the AAM was used for facial feature extraction. An ageing function $age = f(\mathbf{c})$ that relates ages to the vector of facial features \mathbf{c} is defined and used to estimate ages. They proposed that age progression could be realised by inverting the age estimator, $\mathbf{c} = f^{-1}(age)$. However, due to the degenerate nature of the ageing function, its inverse was not computed as proposed. Rather, vectors representing each age group in the training database were saved in a lookup table. To synthesize a face at a new age, they computed the difference $\Delta\mathbf{c}$ between the features in the lookup table. i.e. for current age and new age. Finally, the difference score $\Delta\mathbf{c}$ was subtracted from the subject's original facial feature \mathbf{c} . This technique heavily relies on the training data. In fact, there is no way of rendering the face at an age that is not contained in the database.

In (4), a solution for the inverse problem was proposed. It was also shown that the solution generated photo realistic images, even when the target age did not exist in the training database. However, the ageing function used in (4) was a simple Ordinary Least Squares (OLS) regressor. Unfortunately, OLS has a number of pitfalls which include, outliers, correlation between variables, noisy/irrelevant variables and the curse of dimensionality (17). In general, the performance of OLS degrades as the number of features or variables increase. Hence, we propose an advancement of the work of (4), by improving the ageing function.

Several regression techniques have been proposed for age estimation. These include, Partial Least Squares (PLS) regression, Relevance Vector Machine (RVM) and Support Vector Regression (SVM), to mention a few. For a thorough evaluation of age estimation regression algorithms we refer our reader to (18).

PLS regression is one method that has been widely used for regression as well as dimensionality reduction, especially when the number of variables is large when compared to the observations. Initially, developed in chemometrics, it has been received with considerable interest in other fields which include neuroscience, bioinformatics, social science and recently in computer vision. Although PLS has superior predictability when compared to OLS, recent research (19) has shown that the presence of a large number of variables introduces noise into the PLS latent scores. Hence, Sparse Partial Least Squares (sPLS) regression has been proposed as an improvement to the conventional PLS. Motivated by its predictive power, dimensionality reduction and ability to filter irrelevant variables, we propose to use sPLS at the core of our invertible ageing framework. To the best of our knowledge, while sPLS has been used in other fields, it has never been utilised for age estimation.

Sparse Partial Least Square (sPLS) Regression

Partial Least Squares (PLS) regression was introduced by Wold (20) and has been an alternative to Ordinary Least Squares (OLS) regression. PLS improves OLS in two major ways. They are increased prediction accuracy and enhanced data representation. This statistical method creates latent features via a linear combination of the predictor (X) and response (Y)

variables. Besides regression, it has been applied to classification, dimensionality reduction (21) and data modelling.

Let $\mathbf{x} \in \mathbb{R}^m$ i.e. $\mathbf{X} = \{\mathbf{x}_i\}$ be a matrix of predictor variables whose rows are m dimensional observations and \mathbf{Y} be a matrix of response variables. PLS decomposes the two matrices into,

$$\begin{aligned}\mathbf{X} &= \mathbf{TP}^T + \mathbf{E}, \\ \mathbf{Y} &= \mathbf{TQ}^T + \mathbf{F},\end{aligned}\tag{1}$$

where \mathbf{T} is a matrix composed of k linear latent (scores) vectors, \mathbf{P} and \mathbf{Q} are loadings and \mathbf{E} and \mathbf{F} are matrices of residuals. The scores \mathbf{T} can be computed directly from the feature set \mathbf{X} via,

$$\mathbf{T} = \mathbf{XR},\tag{2}$$

where the matrix of weights $\mathbf{R} = \{\mathbf{r}_1, \mathbf{r}_2, \dots, \mathbf{r}_k\}$ is computed by solving an optimization problem.

The estimate of the k th direction vector is formulated as,

$$\hat{\mathbf{r}}_k = \underset{\mathbf{r}}{\operatorname{argmax}} \mathbf{r}^T \mathbf{X}^T \mathbf{Y} \mathbf{Y}^T \mathbf{X} \mathbf{r} \text{ such that } \mathbf{r}^T \mathbf{r} = 1 \text{ and } \mathbf{r}^T \mathbf{X}^T \mathbf{X} \mathbf{r}_i = 0,\tag{3}$$

for $i = 1 \dots k - 1$.

Thus, PLS captures the directions of highest variance in \mathbf{X} as well as the direction that relates \mathbf{X} and \mathbf{Y} . While many methods for computing PLS have been proposed in the literature, many researchers have embarked on using the classical NIPLAS technique. In this work, however, we shall use the SIMPLS algorithm proposed by De Jong (22), thereby taking the advantage of the speed of the method. Having computed the scores matrix using equation (2), OLS regression of \mathbf{Y} on \mathbf{T} yields the loadings \mathbf{Q} as described in equation (1). Consequently, the PLS regression coefficient is defined as,

$$\beta_{PLS} = \mathbf{RQ}^T.\tag{4}$$

Hence the univariate response variable \mathbf{Y} is formulated as,

$$\mathbf{Y} = \mathbf{X}\beta_{PLS} + \mathbf{F}.\tag{5}$$

As stated earlier, despite the shrinkage ability and efficiency of PLS regression in problems with large number of variables, the fact that it is a linear combination of all variables makes it to include information of both relevant and irrelevant (noisy) data. Recently, Chun and Keles (19)

proposed sparse PLS (sPLS) regression, which integrates sparsity into the conventional PLS dimension reduction procedure. This ensures the selection of only relevant variables. sPLS has proven to be more efficient than PLS when the problem is ill posed. i.e. the number of variables is very large when compared to a small sample size (19).

In order to realise the sPLS regression, the objective function in equation(3) is reformulated by imposing LASSO L_1 regularisation (19,23) on a surrogate direction vector \mathbf{c} , where,

$$\begin{aligned} \min_{\mathbf{r}, \mathbf{c}} \{ & -\kappa \mathbf{r}^T \mathbf{M} \mathbf{r} + (1 - \kappa) (\mathbf{c} - \mathbf{r})^T \mathbf{M} (\mathbf{c} - \mathbf{r}) + \lambda_1 |\mathbf{c}|_1 + \lambda_2 |\mathbf{c}|_2 \} \\ \text{such that, } & \mathbf{r}^T \mathbf{r} = 1, \end{aligned} \quad (6)$$

where $\mathbf{M} = \mathbf{X}^T \mathbf{Y} \mathbf{Y}^T \mathbf{X}$. The L_1 penalty (λ_1) is used to ensure sparsity, while the L_2 tuning parameter (λ_2) is used to avoid singularity in \mathbf{M} . For a univariate predictor \mathbf{Y} , the solution above does not depend on κ and λ_2 . Hence, only λ_1 needs to be tuned. Moreover, it does not have to be explicitly computed for each directional score. Instead, a soft threshold estimate has been formulated in the literature (19). i.e.,

$$\tilde{\mathbf{r}} = (|\hat{\mathbf{r}}| - \eta \max_{1 \leq i \leq p} |\hat{\mathbf{r}}_i|) \mathbf{I}_{(|\hat{\mathbf{r}}| \geq \eta \max_{1 \leq i \leq p} |\hat{\mathbf{r}}_i|)} \text{sign}(\hat{\mathbf{r}}). \quad (7)$$

A different η is required for each directional vector ($i = 1 \dots k$); this is not computationally feasible. Hence, a single sparsity parameter is chosen within the range $0 \leq \eta \leq 1$. Eventually, we only have two parameters to tune the number of components K and the sparsity parameter η .

As stated earlier, sPLS was formulated by Chun and Keles (19), hence, for further details of this method the reader is referred to (19) and (23).

Methodology

Active Appearance Model (AAM)

AAM is a statistical model used for matching the shape and appearance of an object to a target image (14). It is a parameterised model that captures shape and texture variability from a training dataset. Note, "texture" in this context refers to grayscale or colour pixel intensities. The

model provides an avenue for representing the shape and texture of images in terms of few model parameters. Thus, it has proven to be an efficient face abstraction technique.

In order to build the model, a training set of annotated images is formed. Thus, for each face, a number of landmarks is used to mark its key features such as the eyebrows, eyes, nose and mouth. Due to inter-face rotation, translation and scale variations, the Generalised Procrustes Analysis (GAP) (24) is used to align all the landmarks. The set of landmarks representing the face shape is given by,

$$\mathbf{x} = (x_1, x_2, \dots, x_n, y_1, y_2, \dots, y_n)^T, \quad (8)$$

In order to capture the shape variability, principal component analysis (PCA) is used. This means a statistical shape model approximates each face shape x using the linear equation,

$$\mathbf{x} \approx \bar{\mathbf{x}} + \mathbf{P}_x \mathbf{b}_x, \quad (9)$$

where $\bar{\mathbf{x}}$ is the mean shape, \mathbf{P}_x the orthogonal modes of variation and \mathbf{b}_x a set of shape parameters.

To describe the texture \mathbf{g} , “shape free patches” are formed by warping each image to a mean shape. In order to form a colour-based AAM, the three colour channels (red, green and blue) are captured separately and represented as \mathbf{g}_r , \mathbf{g}_g , and \mathbf{g}_b . Research has shown that the three channels are highly correlated, so we used Ohta’s i1i2i3 colour transformation (25) to de-correlate them as follows.

$$\mathbf{g}_1 = (\mathbf{g}_r + \mathbf{g}_g + \mathbf{g}_b)/3, \quad (10)$$

$$\mathbf{g}_2 = (\mathbf{g}_r - \mathbf{g}_b)/2, \quad (11)$$

$$\mathbf{g}_3 = (2\mathbf{g}_g - \mathbf{g}_r - \mathbf{g}_b)/4. \quad (12)$$

To further reduce illumination variations, the above colour textures are normalized using Cootes et al.’s (26) approach of applying a scaling α and an offset β to the texture vectors. To build the statistical texture model, Eigen analysis (27) is applied to equations (10), (11) and (12). The image texture can be approximated by a combination of linear equations such that,

$$\mathbf{g}_1 = \bar{\mathbf{g}}_1 + \mathbf{P}_1 \mathbf{b}_1, \mathbf{g}_2 = \bar{\mathbf{g}}_2 + \mathbf{P}_2 \mathbf{b}_2 \text{ and } \mathbf{g}_3 = \bar{\mathbf{g}}_3 + \mathbf{P}_3 \mathbf{b}_3, \quad (13)$$

where \mathbf{P}_1 , \mathbf{P}_2 , and \mathbf{P}_3 are the orthogonal modes of variations and \mathbf{b}_1 , \mathbf{b}_2 , and \mathbf{b}_3 . Then, equations (9) and (13) are concatenated in a single vector to form the appearance model. Finally, PCA is used to further to de-correlate the shape and texture parameters. The AAM can be approximated using,

$$\mathbf{b} = \mathbf{Q}\mathbf{c}, = \begin{pmatrix} \mathbf{Q}_x \\ \mathbf{Q}_1 \\ \mathbf{Q}_2 \\ \mathbf{Q}_3 \end{pmatrix}, \quad (14)$$

where \mathbf{Q} are eigenvectors, \mathbf{c} is an appearance parameter that controls both shape and texture and can be used as an abstraction of each face in the training dataset. Due to the linear nature of the appearance model, the shape and textures can be expressed in terms of \mathbf{c} , where,

$$\mathbf{x} \approx \bar{\mathbf{x}} + \mathbf{P}_x \mathbf{W} \mathbf{Q}_x \mathbf{c}, \mathbf{g}_i \approx \bar{\mathbf{g}}_i + \mathbf{P}_i \mathbf{Q}_i \mathbf{c}, \quad (15)$$

where $i = 1, 2, 3$ and \mathbf{W} is a diagonal matrix used to compensate the difference in the units of the shapes and the intensities computed using the approach in (4).

Facial Ageing

Research has shown that face shape and texture are a function of age. Hence, it is ideal to build an age estimator by considering a matrix of AAM facial features $\mathbf{C} = \{\mathbf{c}_1, \mathbf{c}_2, \dots, \mathbf{c}_n\}$ as predictors and the column of ages \mathbf{a} as response variables. To this end, an automatic facial age estimator is defined using the sparse PLS regression.

Solving the objective function defined in equation (6), the sPLS weights matrix $\mathbf{R}_{sPLS} = \{\mathbf{r}_1, \mathbf{r}_2, \dots, \mathbf{r}_k\}$ is obtained. Subsequently, this can be substituted into equation (4) in order to get the corresponding sPLS regression coefficients β_{sPLS} . This means the relationship between the AAM features and the univariate ages can be expressed as,

$$\mathbf{a} = \mathbf{C}\beta_{sPLS} + \mathbf{E}, \quad (16)$$

where \mathbf{E} is the sPLS estimation error.

Having modelled the age estimator, age synthesis can be realised by inverting the equation (16). For each face, the feature vector \mathbf{c} is decomposed into two orthogonal components, ageing \mathbf{c}_{age} and identity \mathbf{c}_{id} components. The rationale behind this is fully explained in (4). Hence \mathbf{c} is expressed as,

$$\mathbf{c} = \mathbf{c}_{age} + \mathbf{c}_{id}. \quad (17)$$

The ageing component \mathbf{c}_{age1} at age a_1 is computed using the Moore Penrose Pseudo Inverse,

$$\mathbf{c}_{age1} = \beta_{sPLS}^\dagger a_1. \quad (18)$$

To synthesize a new face, the age component \mathbf{c}_{age2} at the new age a_2 is computed in a similar manner as in equation (18). Following that the identity component \mathbf{c}_{id} is added as shown below,

$$\mathbf{c}_{new} = \mathbf{c}_{age2} + \mathbf{c}_{id}.$$

The shape and texture components of the AAM feature \mathbf{c}_{new} are then computed using equation (15). Finally, an age progressed image is constructed by warping the texture \mathbf{g}_{new} on to the new shape \mathbf{x}_{new} .

Experiments and Results

Data

To test our method, we have used a combined database of 596 high quality color photographs in our experiments. These were acquired from four sources. The first set of 149 images comes from Politecnico di Torino’s “HQFaces” siblings facial images database (28). These images have been captured under controlled lighting conditions, with the subjects’ ages varied between 3 and 50 years. Next, all the 80 images contained in the Dartmouth Children’s Faces Database (29) were obtained. Here, frontal images that were photographed under one lighting condition and displaying neutral facial expression were used. The age range for Dartmouth’s collection is from 6 to 16 years with a 1:1 gender ratio.

Furthermore, 96 images were taken from FGNET-AD aging database. This is made of 1002 face-pictures of 82 people, with each subject having multiple images. Their ages are distributed in the range between 0 and 69. This dataset has varying picture qualities, from grayscale to colour images, having diverse illumination, sharpness and resolution. The subjects in this dataset display varying facial expressions and head pose. The fact that subjects have multiple images taken at different times makes FGNET-AD suitable for initial evaluation of the algorithm.

The remaining 271 images were carefully selected from the Internet, these subjects are mainly well known people, with ages ranging from 1 to 70 years. In total the database has a male to female ratio of 4:3.

With a view to reducing computational cost, all 596 images were cropped to 340 x 340 pixels. Next, we annotated each image with 79 landmarks using the approach of (30), as shown in Fig. 1. Note, the landmarks were aligned using GAP. This was done to eliminate rotational, translational and scaling variations.



Fig. 1: Face shape captured using landmarks (a) Position of 79 landmarks (b) Unaligned face shapes (c) Shapes aligned using GPA.

Experimental Set-up

All experiments were performed on a PC with a 64-bits Windows 10 Operating System, Intel Core i7-6700T CPU, 8 MB Cache, 2.8 GHZ Clock Speed and 16 GB RAM. Active appearance model (AAM) feature extraction and image reconstruction algorithms were implemented in MATLAB R2014b (Version 8.4). Furthermore, CRAN 'spl' Package Version 2.2-1 (31) was used for the implementation of sparse partial least squares regression.

Age Estimation Experiment

The colour based AAM described in Section 3 was trained with the images in our database. As a result, each face was represented by a vector \mathbf{c} having $n - 1$ elements, where n is the number of samples ($n = 596$). It is worth noting that the AAM usually reduces the number of components by 1, because PCA - which is at the core of the model - produces $(n - 1)$ eigenvalues that are

larger than 0. In a nutshell, using the AAM, each 340 x 340 pixels image is now represented by a vector of numbers, whose dimension is $(n - 1) \times 1$.

An automatic age estimator was then built using sPLS regression model explained in (16). Here, sPLS tuneable parameters K and η are selected via 10 fold cross-validation. To be precise the values used for this experiment are, $K=27$ and $\eta =0.7$. For the purpose of comparison and evaluation, two other age estimators were modelled using PLS and OLS regressions.

In order to evaluate the accuracy of estimation, we employed Leave One Person Out (LOPO) cross validation method [4]. For each fold, the image of 1 person is used as the test set and an estimator is trained using the remaining subjects. Thus, by the end of n folds each subject will have been used for testing. Finally all n separate estimations are averaged. The performance measures used are Mean Absolute Error (MAE) and Cumulative Score (CS), expressed as,

$$MAE = \sum_{i=1}^N |a - a'| / N,$$

$$CS(m) = N_{error \leq k} / N \times 100\%, \quad (19)$$

where a is the ground truth age and a' is the estimated age, N the number of images (i.e. 596) and $N_{error \leq k}$ denotes the number of images on which the system makes absolute error not higher than k years. In our experiment, we chose a value of $k = 10$ inline with state of the art literature. The results of the above evaluations are tabulated and illustrated in Table 1 and Fig. 2 respectively. It has been observed that both sPLS and PLS outperform the OLS method. Furthermore, our sPLS regression estimator improves on the result of PLS regression by achieving a mean absolute error of 5.53 as opposed to 5.68. It is also obvious that using sPLS, over 86% of the dataset achieved an estimation error of less than 10 years.

Table 1: Results of age estimation experiments.

Algorithm	MAE	CS < 10
OLS	7.72	73.33%
PLS	5.68	84.54%
sPLS	5.53	86.92%

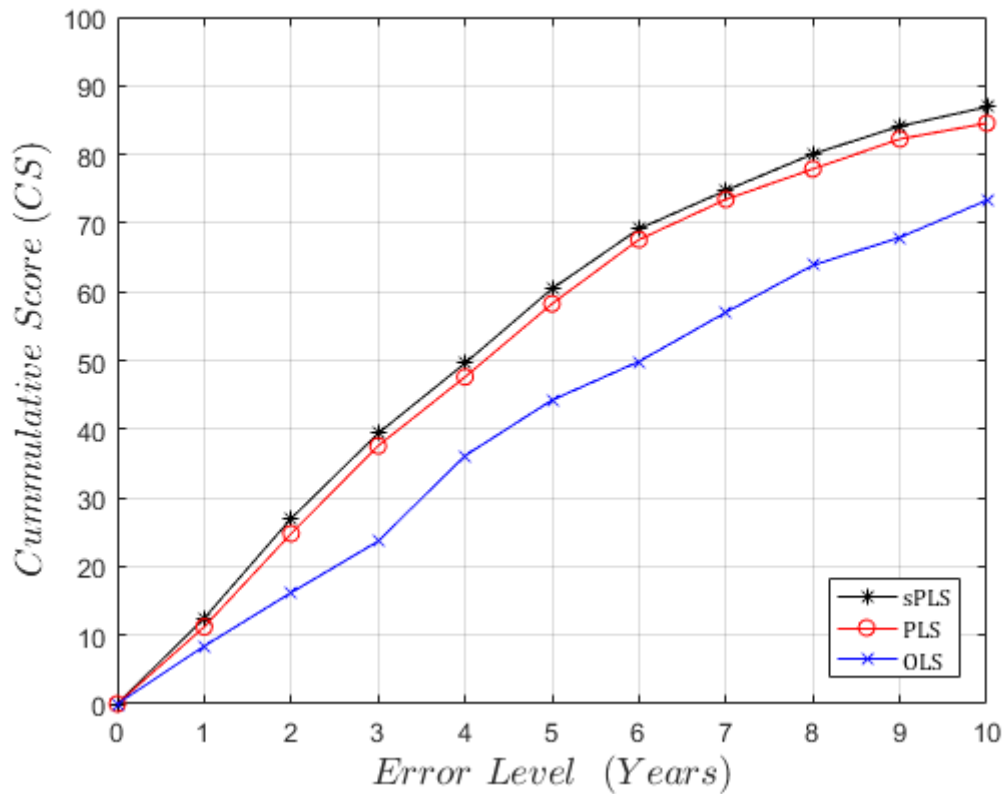


Fig. 2: CS at error levels from 0 -10 years.

Age Progression Results

To fully evaluate the performance of our synthesis algorithm, we conducted extensive experiments on images of people with multiple pictures taken at different times of their lives. For this purpose we chose the images we extracted from the FGNET-AD, since this gave us the opportunity to compare our synthesized results to real images at the same age. Results of this initial experiment are shown in Fig. 2. Images on the left most column are the test images, columns 2 and 4 are the subjects' real images at the projected age, while images on columns 3 and 5 are the corresponding images synthesized by our method.

Next, we used the same ageing framework to progress the image of Ben Needham to the ages of 6, 14, and 22 years as shown in Fig. 3. By compositing, external features such as hair and ears were then added to the generated images as shown in Fig. 4. Subsequently, the images we synthesised are compared to the existing Police generated images as shown in Fig. 5.

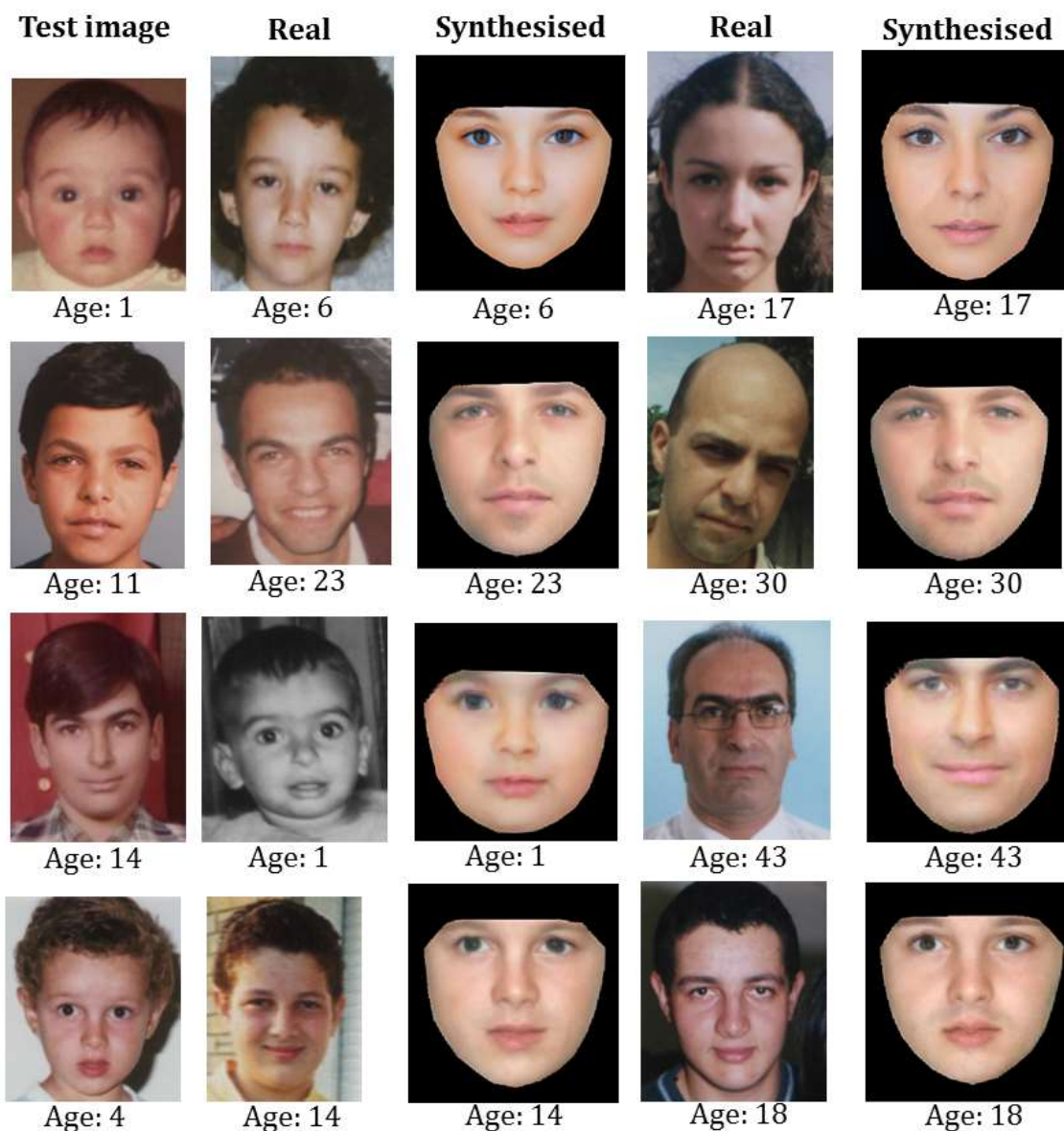


Fig. 3: Evaluation of synthesis algorithm on known subjects.

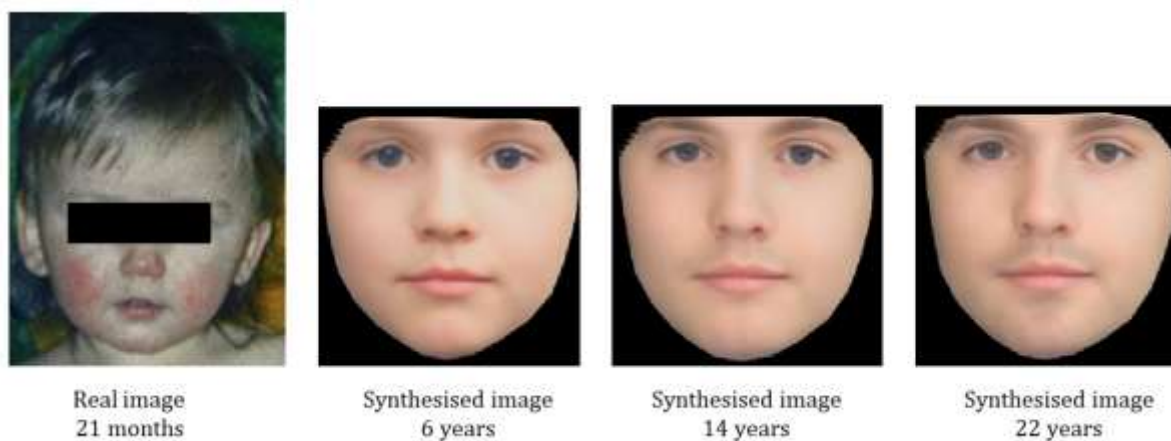


Fig. 4: Synthesised images of Ben Needham.

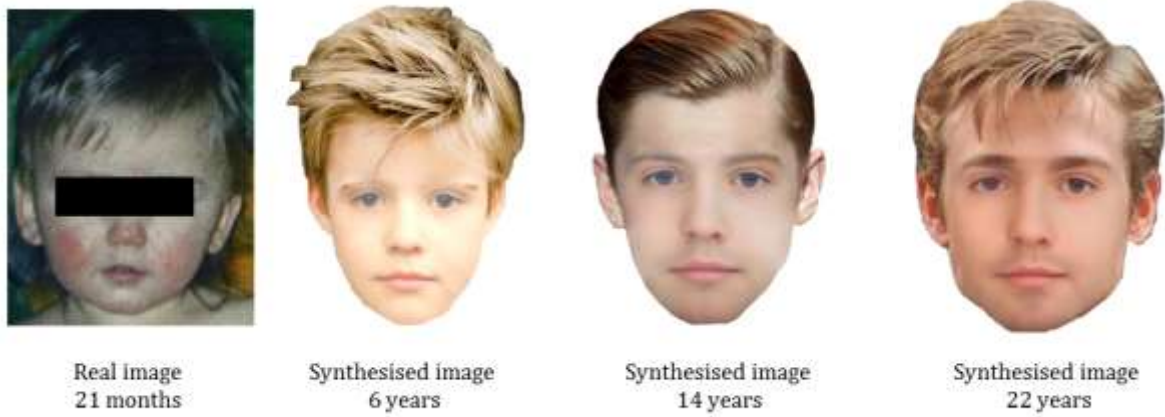


Fig. 5: External facial features incorporated on synthesised images via compositing.



Fig. 6: Existing Police generated images of Ben Needham.

Analysis

An effective means of assessing facial age progression should have two main features. They are evaluating the ability to synthesize images that fit the intended age and checking the ability to retain the identity of the subject in age altered images. There are two ways we can perform the evaluations. They are machine based and human based methods (2). In our experiment, both methods were utilised.

Given two images p_1 and p_2 , having AAM-facial features c_{p_1} and c_{p_2} , the machine based test conducted using Euclidean Distance (ED) of the AAM-facial features is expressed as,













$$ED = \sqrt{\sum (c_{p_1} - c_{p_2})^2}, \quad (20)$$

The ED gives us a value between 0 and 1 which describes how similar two images are; the closer the value is to 1 the more the similarity. Consequently, it is then possible to compute a similarity score (Sc) as defined by Segaran (32) that converts the ED into a percentage metric such that a score of 100% denotes best match. Thus, we define Sc as,

$$Sc = \frac{1}{1+ED} \times 100\%. \quad (21)$$

For the first experiment, we computed Sc between the test image and our synthesized images to show the degree to which our algorithm reserves the subject's identity. Results of this test are presented in Table 2. Values close to 100 denote very close match between the real image and the synthesized image. Obviously, most of the images generated using the proposed procedure have high Sc thus indicating the age-progressed images resemble the real pictures, thus the person's identity is retained.







Table 2: Machine-based evaluation of initial experiments.

Test Image	Sc for Synthesized Image 1	Sc for Synthesized Image 2
	 79.65%	 79.49%
	 96.25%	 96.22%
	 77.07%	 96.00%
	 98.21%	 98.19%

In order to evaluate our method on Ben's images we compared our results to those produced by the Metropolitan Police. A machine based test as described in the first experiment was performed. Here Sc was computed between Ben's real image and each of the age-progressed images (ours and those of the Police). The results were then ranked based on shortness of

Euclidean Distance, as shown in see Table 3. It is worth noting that the shorter the ED, the closer the similarity score Sc is to 100%.

Table 3: Evaluation of Ben Needham's images.

Synthesized Image	Ranks Based on ED	Mean Rank Human Test
	1	2.19
	3	2.84
	2	3.11
	4	3.23
	5	4.15
	6	4.77

Next, a human based test was conducted. In it, 29 observers were shown Ben's real image as well as the synthesized images. Then, each person was asked to rank the images based on their similarity to the original photograph, i.e. a position of 1 is assigned to the image that resembles the subject the most, 2 to the next and so on. Finally, the 29 rankings were averaged in order to decide which picture was perceived to look more like Ben. As can be seen in Table 2, the results show that images generated using our method look more like the missing toddler.

Discussion and Conclusion

We have presented a new approach to facial age synthesis, using sPLS. In addition to the good qualities of the conventional PLS which include dimensionality reduction and increased prediction accuracy, sPLS imposes sparsity on the variables. This ensures only relevant variables are encoded into the regressor. Using sPLS, an age estimation model with good predictive power is first modelled. Then, a method of inverting the age estimator is developed.

This was then used to generate aged faces. Results show that plausible images can be rendered at different ages automatically using the inverted model.

We have used our method in a real life scenario, i.e. the case of Ben Needham. We generated aged images of the subject using our method and compared them to those produced by the Police. Our method provides different predictions of the face. Although the police have closed the case, we are advocating our improved method to aid police work in future cases and perhaps even for Ben Needham as we hope these new images are closer to his present day appearance.

Due to variations in hair style and the fact that some of the images in our database have occluded ears, we did not consider hair and ears in our synthesis framework. However, as stated earlier, external facial features were incorporated to the synthesized images via compositing. This was done for cosmetic or enhanced visualisation purposes. We want to point out that this is highly subjective and might alter the visual look of the real results. In order to fully incorporate these external features, it will be necessary to thoroughly study and develop further automated methods that can incorporate such external facial features.

Clearly, our work leaves room for future improvements. With a view to improving image rendering, an efficient method of incorporating external features should be investigated. Thus, using existing ear biometric methods, our age synthesis framework could be improved by incorporating the human ear. Other external features can be incorporated in a similar fashion. Furthermore, at this moment in time, our facial landmarks are annotated manually. This is indeed a laborious task. Therefore, it will prove useful to develop fully automatic methods for facial landmark annotations.

References

1. Needham K. Ben. London: Ebury Publishing; 2013.
2. Fu Y, Guo G, Huang T. Age Synthesis and Estimation via Faces : A Survey. *IEEE Trans Pattern Anal Mach Intell.* 2010;32(11):1955–76.
3. Fyfe NR, Stevenson O, Woolnough P. Missing persons: the processes and challenges of police investigation. *Polic Soc.* 2015;25(4):409–25.
4. Bukar AM, Ugail H, Connah D. Individualised Model of Facial Age Synthesis Based on Constrained Regression. In: *Image Processing Theory, Tools and Applications (IPTA), 2015 5th International Conference on.* IEEE; 2015. p. 285–90.
5. Panis G, Lanitis A, Tsapatsoulis N, Cootes TF. Overview of research on facial ageing using the FG-NET ageing database. *IET Biometrics.* 2015;
6. Patterson E, Sethuram A, Albert M, Ricanek K. Comparison of synthetic face aging to age progression by forensic sketch artist. In: *International Conference on Visualization, Imaging, and Image Processing.* Palma de Mallorca, Spain; 2007. p. 247–52.
7. Kwon YH, Lobo V. Age classification from facial images. *Proc IEEE Conf Comput Vis Pattern Recognit CVPR-94.* 1994;762–7.
8. Hsu R, Jain AK. Using Interacting Snakes. *IEEE Trans Pattern Anal Mach Intell.* 2003;25(11):1388–98.
9. Waters K. A muscle model for animation three-dimensional facial expression. *ACM SIGGRAPH Comput Graph.* 1987;21(4):17–24.
10. Lee Y, Terzopoulos D, Walters K. Realistic modeling for facial animation. *Proc 22nd Annu Conf Comput Graph Interact Tech SIGGRAPH 95.* 1995;95:55–62.
11. Hayashi J, Yasumoto M, Ito H, Koshimizu H. Method for estimating and modeling age and gender using facial image processing. *Proc Seventh Int Conf Virtual Syst Multimed.*

- 2001;439–48.
12. Mukaida S, Ando H. Extraction and manipulation of wrinkles and spots for facial image synthesis. Sixth IEEE Int Conf Autom Face Gesture Recognition, 2004 Proceedings. 2004;749–54.
 13. Mehdi A, Qahwaji R, Ugail H, Abdullah M. Construction of 3D Facial Wrinkles using Splines. In: Fourth International Conference on Information Technology. Jordan; 2009.
 14. Cootes TF, Edwards GJ, Taylor CJ. Active Appearance Models. 2001;23(6):681–5.
 15. Zhang L, Wang S, Samaras D. Face synthesis and recognition from a single image under arbitrary unknown lighting using a spherical harmonic basis morphable model. Proc IEEE Comput Soc Conf Comput Vis Pattern Recognit. 2005;2:209–16.
 16. Lanitis A, Taylor C, Cootes T. Toward Automatic Simulation of Aging Effects on Face Images. IEEE Trans Pattern Anal Mach Intell. 2002;24(4):442–55.
 17. Bluman AG. Elementary Statistics: A Step By Step Approach. 2007;604.
 18. Fernandez C, Huerta I, Prati A. A Comparative Evaluation of Regression Learning Algorithms for Facial Age Estimation. FFER conjunction with ICPR, Press IEEE. 2014;
 19. Chun H, Keleş S. Sparse partial least squares regression for simultaneous dimension reduction and variable selection. J R Stat Soc Ser B (Statistical Methodol. 2010;72(1):3–25.
 20. Wold H. Quantitative sociology: international perspectives on mathematical and statistical model building, chapter path models with latent variables: the NiPALS Approach. Academic, London; 1975. 307-357 p.
 21. Khedher L, Ramírez J, Górriz JM, Brahim A, Segovia F. Early diagnosis of Alzheimer's disease based on partial least squares, principal component analysis and support vector machine using segmented MRI images. Neurocomputing. 2015;151:139–50.

22. De Jong S. SIMPLS: An alternative approach to partial least squares regression. *Chemom Intell Lab Syst* [Internet]. 1993;18(3):251–63. Available from: <http://www.sciencedirect.com/science/article/pii/016974399385002X>
23. Chun H. *Sparse Partial Least Squares Regression for Simultaneous Dimension Reduction and Variable Selection with Applications to High Dimensional Genomic Data*. Michigan: ProQuest; 2008.
24. Gower JC. Generalized procrustes analysis. *Psychometrika*. 1975;40(1):33–51.
25. Ohta YI, Kanade T, Sakai T. Color Information for Region Segmentation. *Comput Graph Image Process*. 1980;13(1):222–41.
26. Cootes TF, Edwards GJ, Taylor CJ. Active Appearance Models. In: *In Computer Vision—ECCV'98* [Internet]. 1998. p. 484–98. Available from: <http://link.springer.com/chapter/10.1007/BFb0054760>
27. Turk MA, Pentland AP. Eigenfaces for recognition. *J Cogn Neurosci*. 1991;3(1):71–86.
28. Vieira TF, Bottino A, Laurentini A, De Simone M. Detecting siblings in image pairs. *Vis Comput*. 2014;30(12):1333–45.
29. Dalrymple KA, Gomez J, Duchaine B. The dartmouth database of children's faces: Acquisition and validation of a new face stimulus set. *PLoS One*. 2013;8(11):1–7.
30. Bukar AM, Ugail H, Connah D. Automatic age and gender classification using supervised appearance model. *J Electron Imaging*. 2016;25(6):1–11.
31. Chung D, Chun H, Keles S. *Spls: Sparse partial least squares (SPLS) regression and classification*. R Packag version 2. 2012;2:1.
32. Segaran T. *Programming collective intelligence: building smart web 2.0 applications*. "O'Reilly Media, Inc."; 2007.